Combined Sparsifying Transforms for Compressive Image Fusion

Chen WU[1], Haixian WANG[2], Xinzhou XU[1], Li ZHAO[1]
[1]*Key Laboratory of Underwater Acoustic Signal Processing of Ministry of Education, Southeast University, 210096, China*
[2]*Key Laboratory of Child Development and Learning Science of Ministry of Education, Southeast University, 210096,China*
230129135@seu.edu.cn

***Abstract*—In this paper, we present a new compressive image fusion method based on combined sparsifying transforms. First, the framework of compressive image fusion is introduced briefly. Then, combined sparsifying transforms are presented to enhance the sparsity of images. Finally, a reconstruction algorithm based on the nonlinear conjugate gradient is presented to get the fused image. The simulations demonstrate that by using the combined sparsifying transforms better results can be achieved in terms of both the subjective visual effect and the objective evaluation indexes than using only a single sparsifying transform for compressive image fusion.**

***Index Terms*—compressive sensing, combined sparsifying transforms, image fusion.**

I. Introduction

Compressive sensing (CS) [1-2] is a recently developed theory and has been widely used in many applications such as compressive imaging [3-4], speech coding [5-6], and biomedical signal processing [7-8] etc. It demonstrates that a sparse or compressible signal can be accurately reconstructed from a small number of incoherent projections, which is far fewer than the number of samples if the signal is sampled at the Nyquist rate [9]. CS theory provides the possibility of reconstructing the signal at a lower sampling rate without any prior information about the observed signal. It thus can significantly reduce the storage space and simplify the sampling hardware.

All the advantages of CS discussed above motivate us to combine image fusion application with CS theory in order to reduce the burden at the sensor side. Wan et al. firstly proposed an image fusion framework based on CS theory in [10-11]. They use the spatial finite-difference as the sparsifying transform and Min-TV (Total Variation) as the reconstruction model in those papers. Meanwhile, the fusion rule employed there is the maximum of absolute value (MAV). As the spatial finite-difference is not a good sparsifying transform for natural images [12], wavelet transform is used in place of it in [13] and the reconstruction model used there is Min-L1. Moreover, although MAV fusion rule has been widely used in wavelet based image fusion framework, it doesn't work very well in compressive image fusion. As a result, linear fusion scheme via the weighted average on the CS measurements is proposed in [12-13], which proves to be more reasonable. In [12], the weights are calculated based on standard deviation (SD) of the CS measurements. And a different fusion rule is proposed in [13], where the weights are calculated based on entropy metrics of the CS measurements.

Combined sparsifying transforms is used in [14] for CS based Magnetic Resonance (MR) imaging to improve the sparsity of MR images. Inspired by this, we propose a new compressive image fusion method based on combined sparsifying transforms to improve the compressive image fusion results. Three different sparsifying transforms: the spatial finite-difference, the wavelet and the contourlet are employed for sparsely representing different features of images. As a consequence, the reconstruction model becomes combined Min-TV and Min-L1. We also present a reconstruction algorithm based on the nonlinear conjugate gradient to get the fused image.

The rest of this paper is organized as follows. Section II provides a brief review of the framework of compressive image fusion. In Section III, our proposed compressive image fusion scheme is presented. Simulation results are given in Section IV. Finally, conclusion and suggestions for future work are given in Section V.

II. Framework of Compressive Image Fusion

The framework of compressive image fusion is illustrated in Fig. 1. It consists of four steps: (1) finding a sparsifying transform to sparsely represent the input images; (2) taking the compressive measurements of the input images; (3) using the fusion rule to fuse the compressive measurements into a composite one; (4) getting the fused image via CS reconstruction algorithm. Below, we will discuss the four steps in details.

A. Sparsifying transform

Sparse is the core concept of the CS theory, the sparser of the signal, the fewer measurements we should take. For a signal x with length N (an image can be vectorised into a long one-dimensional vector), we say x is K sparse if it can be represented as

$$x = \Psi \alpha \tag{1}$$

where Ψ is the sparsifying transform and α is a vector containing only $K<<N$ nonzero coefficients.

In previous work of compressive image fusion, the spatial finite-difference is commonly used as the sparsifying

This work was supported in part by the National Science Foundation of China under Grant No. 61231002, No. 61273266 and No. 51075068 and the Doctoral Fund of Ministry of Education of China under Grant No. 20110092130004.

Digital Object Identifier 10.4316/AECE.2013.04014

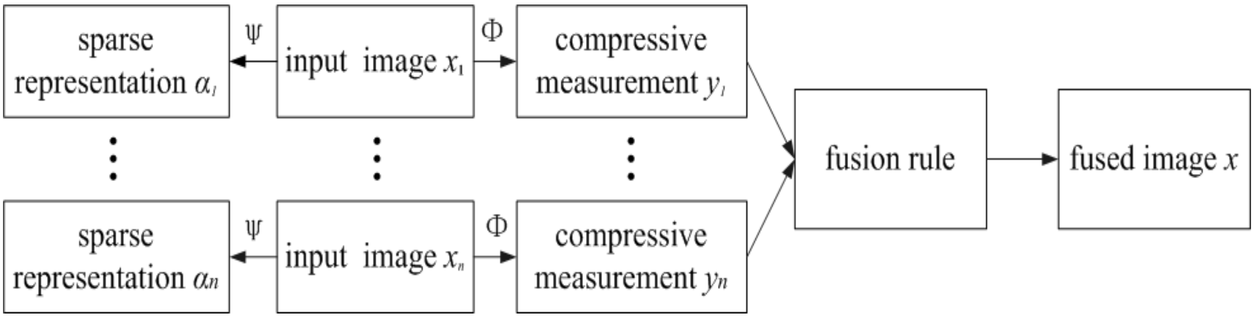

Figure 1. The framework of compressive image fusion

transform in [10-12]. As the spatial finite-difference is not a good sparsifying transform for natural images [12], wavelet transform is used in place of it in [13]. However, the spatial finite-difference can only sparsely represent piecewise smooth images and the wavelet transform is good at sparsely representing point-like features but fails in sparsely representing curve-like features [14]. So in section III, we consider use the combined sparsifying transforms in order to improve the sparsity of the input images.

B. Compressive measurements

In CS, we take the compressive measurements via:

$$y = \Phi x = \Phi \Psi \alpha \tag{2}$$

where Φ is a M×N measurement matrix and y is a vector with length M. Although M<N makes the recovery of x from the compressive measurements y an ill-conditional problem, it is shown that a sparse signal can be recovered perfectly if Φ satisfies the restricted isometry property (RIP) [1- 2].

There exist different ensembles of matrices that satisfy the RIP, for example the random Gaussian matrix [1], the uniform Spherical ensemble [2] and partial Fourier matrix [10-12] etc. In this paper, we adopt the star-shaped sampling pattern in the 2D Fourier plane as in [12]. An example of the star-shaped sampling pattern is shown in Fig. 2. White lines here indicate the locations to be sampled. We choose more samples near the centre and fewer samples near the corner owing to the fact that input images usually contain much more low-frequency information than high-frequency information. For obtaining different measurement numbers, we can easily change the density of the sampling lines.

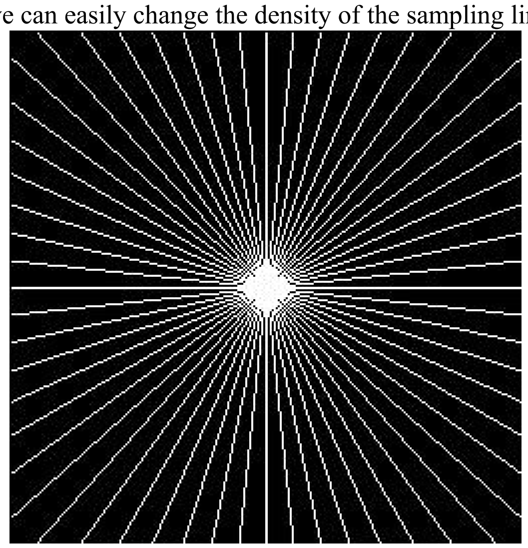

Figure 2. Star-shaped sampling pattern

C. Fusion rule

After having taken the compressive measurements of input images, we should choose a fusion rule to fuse the compressive measurements into a composite one.

Maximum of absolute value (MAV) is used as the fusion rule in [10-11]. Although the MAV fusion rule has been successfully used in the transform-based image fusion framework, it doesn't work very well in the compressive image fusion application. That is because in compressive image fusion framework, after sampling the input images via a compressive measurement matrix, coefficient with larger value does not mean it contains more information as in the traditional transform-based image fusion framework. To overcome the drawbacks, weighted linear fusion rule is proposed in [12-13], which proves to be more reasonable. In [12], the weights are calculated based on standard deviation (SD) of the compressive measurements. Meanwhile, a different fusion rule is adopted in [13], where the weights are calculated based on entropy metrics of the compressive measurements.

In this paper, we adopt the weighted linear fusion rule based on SD of the compressive measurements. An image with larger SD has more dispersed grey scale and usually contains more information accordingly [12]. For compressive measurements $y_1,\ldots\ldots,y_n$, we first calculate the weights

$$w_i = sd_i \,/ \sum_{k=1}^{n} sd_k \tag{3}$$

where sd_i is SD of the compressive measurements y_i defined as

$$sd_i = \frac{1}{M}\sum_{k=1}^{M}(y_i[k] - \frac{1}{M}\sum_{j=1}^{M} y_i[j]) \tag{4}$$

Then, the composite measurements y can be acquired via

$$y = \sum_{i=1}^{n} w_i y_i \tag{5}$$

D. Reconstruction algorithm

Although M<N makes the recovery of the fused image from the composite measurements y ill-posed, it is possible to solve it with efficient algorithms recently developed in CS literatures. In previous compressive image fusion papers, [10-12] use the Min-TV optimization algorithm [1] and the gradient projection for sparse reconstruction (GPSR) algorithm [15] is employed in [13] to solve the Min-L1 problem. In this paper, we use the reconstruction algorithm based on the nonlinear conjugate gradient to solve the combined Min-TV and Min-L1 problem, which will be

introduced in section III.

III. Our Proposed Scheme

A. Combined sparsifying transforms

In previous compressive image fusion work, the spatial finite-difference and the wavelet transform are used as the sparsifying transform in [10-12] and [13], respectively. However, single sparsifying transform cannot sparsely represent all features of the input images, which limits the reconstruction quality of the fused image. The spatial finite-difference transform can sparsely represent piecewise smooth images, but for natural images this assumption does not always exist. The wavelet transform is good at sparsely representing point-like features but fails in sparsely representing curve-like features [14].

Combined sparsifying transforms are proposed in [14] for CS based MR imaging to improve sparsity of the MR images. Following this line, we propose a new compressive image fusion method based on combined sparsifying transforms to improve the quality of the fused image. Because the contourlet transform [16-17] is good at sparsely representing curve-like features and has been successfully used in transform-based image fusion framework [18], we consider using it as a complement transform. So In this paper, we combine the spatial finite-difference transform, the wavelet transform and the contourlet transform simultaneously to improve the reconstruction quality of the fused image.

B. Reconstruction model

When using the spatial finite-difference transform, the reconstruction model to get the fused image is Min-TV [10-12]

$$\arg\min_{x} TV(x) \qquad \mathrm{st.}\Phi x = y \tag{6}$$

where TV(x) is defined as

$$TV(x) = \sum_{i,j} \sqrt{(D_1 x_{ij})^2} + \sqrt{(D_2 x_{ij})^2} \tag{7}$$

where D_1 and D_2 denote the forward finite-difference operators on the row and column directions, respectively.

For wavelet transform, the reconstruction model is Min-L1, which is defined as

$$\arg\min_{x} \|\Psi x\|_1 \qquad \mathrm{st.}\Phi x = y \tag{8}$$

where Ψ denote the wavelet transform.

In this paper, with the combined sparsifying transforms, we use the following reconstruction model

$$\arg\min_{x} \beta TV(x) + \lambda_1 \|\Psi_1 x\|_1 + \lambda_2 \|\Psi_2 x\|_1 + \frac{1}{2}\|\Phi x - y\|_2 \tag{9}$$

where Ψ_1 and Ψ_2 denote the wavelet transform and the contourlet transform, respectively. β, λ_1 and λ_2 are all parameters that trade the signal sparsity with data consistency.

C. Reconstruction algorithm

To get the fused image x via the composite measurements y, we should use reconstruction algorithm to solve the reconstruction model. An algorithm based on the nonlinear conjugate gradient descent with backtracking line search technique is proposed for CS based MR imaging [19-20]. Here, we modify it to solve the reconstruction model defined in (9). Details of the algorithm are shown in Algorithm 1.

Algorithm 1
Input parameters: f (x)-- cost function defined as (9) maxIter--stopping criteria by number of iterations α,δ--line search parameters μ--positive smoothing parameter

Initialization:
$k=0$
$x_0 = 0$
$g_0 = \nabla f(x_0)$
$\Delta x_0 = -g_0$
Iterations:
while($k \le \max Iter$)
{
t=1;
while($f(x_k + t\Delta x_k) > f(x_k) + \alpha t \bullet \mathrm{Real}(g_k^* \Delta x_k)$)
{
$t = \delta t$
}
$x_{k+1} = x_k + t\Delta x_k$
$g_{k+1} = \nabla f(x_{k+1})$
$\gamma = \|g_{k+1}\|_2^2 / \|g_k\|_2^2$
$\Delta x_{k+1} = -g_{k+1} + \gamma \Delta x_k$
$k = k+1$
}

outputs: the fused image x

In Algorithm 1, the conjugate gradient of the cost function f (x) is defined as

$$\nabla f(x) = \Phi^*(\Phi x - y) + \sum_{i=1}^{2}(\lambda_i \Psi_i^* W_i^{-1} \Psi_i x + \beta D_i^* \Lambda_i^{-1} D_i x) \tag{10}$$

where superscript * of a matrix denotes the adjoint operator, W_i is a diagonal matrix with diagonal elements defined as

$$w_i = \sqrt{(\Psi_i x)^* (\Psi_i x) + \mu} \tag{11}$$

and Λ_i is also a diagonal matrix with diagonal elements defined as

$$\xi_i = \sqrt{(D_i x)^* (D_i x) + \mu} \tag{12}$$

The convergence property of the nonlinear conjugate gradient descent has been given in [21]. Moreover, when incorporating backtracking line search technique, update step-size can be adaptively determined in each iteration. However, the number of iterations for nonlinear conjugate gradient descent method also varies with different factors, such as initial solution, problem size, desired accuracy, line search parameters, sampling ratio [19], and in our problem, also the speed of FFT, wavelet and contourlet transforms. An experiment test showed that, with our algorithm carried out in MATLAB on a laptop with 4GB memory, images of size 256×256 can be fused within 25 seconds, and images of size 512×512 can be fused within 40 seconds.

D. Compressive image fusion procedure

The whole procedure of the presented compressive image

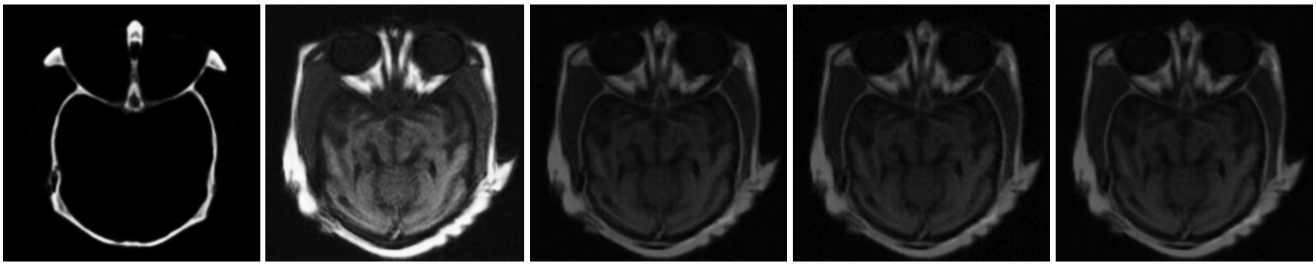

(a) (b) (c) (d) (e)

Figure 3. Fusion results for *Med* (M/N=30%): (a) and (b) input source images, (c) fused image of finite-difference transform method, (d) fused images of wavelet transform, (e) fused image of our presented method

(a) (b) (c) (d) (e)

Figure 4. Fusion results for *Clock* (M/N=30%): (a) and (b) input source images, (c) fused image of finite-difference transform method, (d) fused images of wavelet transform, (e) fused image of our presented method

fusion framework based on combined sparsifying transforms is summarized as follows:

Step 1: taking the compressive measurements y_i of input image x_i via

$$y_i = \Phi x_i \quad i = 1,\ldots\ldots, \; n \tag{13}$$

where matrix Φ denotes the star-shaped sampling pattern in the 2D Fourier plane.

Step 2: fusing the acquired compressive measurements $y_1,\ldots\ldots,y_n$ into a composite measurements y using the weighted linear fusion rule based on SD of the compressive measurements via (3), (4) and (5).

Step 3: reconstructing the fused image x from the composite measurements y with Algorithm 1.

IV. Simulation and Results

Two sets of test images are employed for fusion performance evaluation. For the multi-focus images Clock (512×512), one image focuses on the small clock while the other focuses on the big clock. For medical images Med (256×256), one is a CT image while the other is captured by MRI.

In our simulations, parameters used in Algorithm 1 are set as: maxIter=100, α=0.01, δ=0.6, $\mu=1\times10^{-15}$, $\beta=1\times10^{-3}$, $\lambda_1=\lambda_2=1.5\times10^{-3}$. We compare our presented algorithm with the single sparsifying transform based compressive image fusion algorithm. When using only a single spatial finite-difference transform (TV), we generally set $\lambda_1=\lambda_2=0$ in Algorithm 1. And we set $\beta=\lambda_2=0$ for single wavelet transform based compressive image fusion method.

Fig. 3 and Fig. 4 illustrate the compressive image fusion results of the two test image sets with only 30% of the Fourier coefficients. We can see that all compressive sensing based image fusion methods can give faithful fusion performance using only 30% of the Fourier coefficients of input images, which demonstrates the potential of the compressive sensing based image fusion framework for lighting the complexity on the sensor side. However, fused image obtained by our presented method contains more detailed information and has higher contrast compared with a single sparsifying transform based compressive image fusion method.

In addition to visual comparison, we also compare the compressive image fusion performance with two objective metrics: mutual information (MI) [22] and edge preservation (EP) [23].

MI [22] evaluates the mutual information between the fused image x and input images a and b, which is defined as

$$MI = I(x,a) + I(x,b) \tag{14}$$

where I(x,a) and I(x,b) is given by

$$I(x,a) = \sum p(x,a)\log_2 \frac{p(x,a)}{p(x)\,p(a)} \tag{15}$$

$$I(x,b) = \sum p(x,b)\log_2 \frac{p(x,b)}{p(x)\,p(b)} \tag{16}$$

where p(x) is the normalized histogram of the fused image x, p(x,a) are the joint distribution of the fused image x and the input image a, and p(x,b) are the joint distribution of the fused image x and the input image b. Larger values of MI indicate better image fusion quality that the fused image can pick up more information from input images.

EP [23] assessments the relative amount of edge information conveyed from input images into the fused image, which is defined as

$$Q = \frac{\sum_{n=1}^{N}\sum_{m=1}^{M} Q^a(n,m)w^a(n,m) + Q^b(n,m)w^b(n,m)}{\sum_{n=1}^{N}\sum_{m=1}^{M}(w^a(n,m) + w^b(n,m))} \tag{17}$$

where

$$Q^a(n,m) = Q_e^a(n,m)\,Q_o^a(n,m) \tag{18}$$

where $Q_e^a(n,m)$ and $Q_o^a(n,m)$ denote the edge strength and orientation preservation values at the pixel (n,m), respectively. The definition of $Q^b(n,m)$ is the same as $Q^a(n,m)$, which uses the values of the input image b instead of the values of the input image a in (17) and (18). $w^a(n,m)$ and $w^b(n,m)$ denote the significance of $Q^a(n,m)$

and $Q^b(n,m)$, respectively. The range of Q is in [0, 1]. Larger values of EP imply that the fused image preserves more edge information.

The fused performances of Fig. 3 and Fig. 4 in terms of MI and EP metrics are tabulated in Table 1. It is shown that compressive image fusion scheme achieves better performance when using combined sparsifying transforms than using only a single sparsifying transform. Meanwhile, we can also see that, for a single sparsifying transform, the spatial finite-difference transform get better performance than the wavelet transform, which coincides with the results in [12].

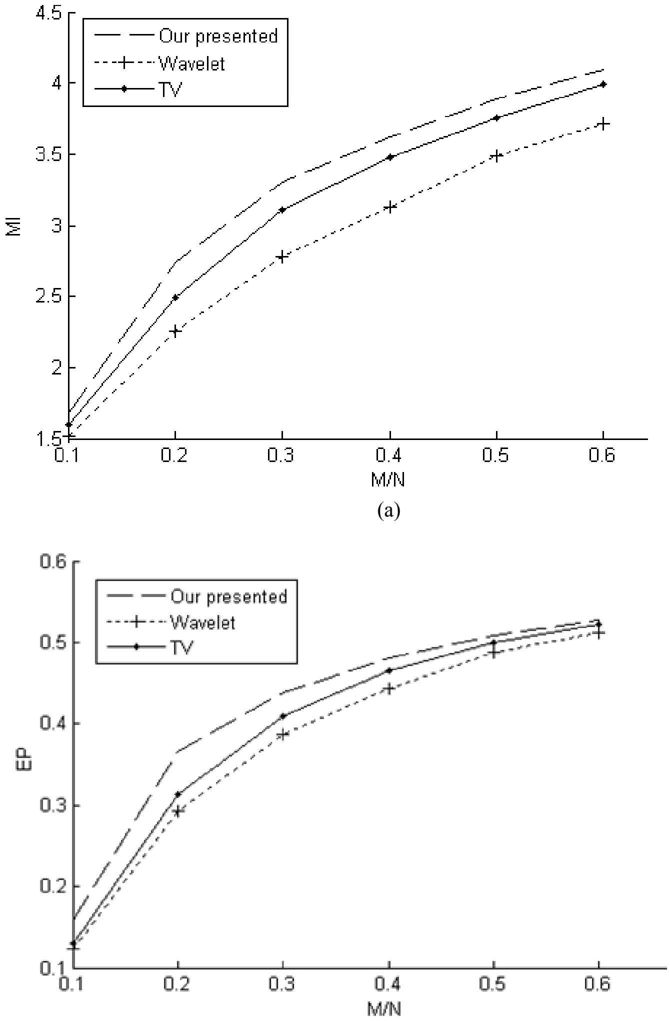

Figure 5. Objective metrics results of different methods for Med: (a) mutual information (MI), (b) edge preservation (EP)

We also test the fused performance of different image fusion methods with different sampling ratio in terms of MI and EP. Results of Med and Clock are shown in Fig.5 and Fig.6, respectively. Again, we can see clearly that our presented method outperforms single sparsifying transform based methods and the spatial finite-difference transform (TV) based method gives better results than the wavelet transform based method. We also notice that, with the increasing sampling ratio, all the compressive image fusion methods achieve better results. When the sampling ratio grows up to 60%, the differences between all the compressive image fusion methods become negligent, which can also be observed in conventional compressive sensing studies. As stated in [1-2], a K sparse signal can be exactly reconstructed by more than 3K measurements. It implies that 60% sampling ratio is sufficient for all the compressive image fusion algorithms. However, for lower sampling ratio, our presented method can give significantly better results than single sparsifying transform based methods because of the sparser representation of input images that benefit from the combined sparsifying transforms.

V. Conclusion and Future Work

In this paper, we present a compressive image fusion scheme based on combined sparsifying transforms. First, we provide a brief introduction of the framework of compressive image fusion. Then, combined sparsifying transforms are presented to enhance the sparsity of images. Finally, a reconstruction algorithm based on the nonlinear conjugate gradient is presented to get the fused image. Simulations demonstrate that compressive sensing based image fusion framework can effectively fuse the images from fewer measurements without any prior information about the input images. Therefore, compressive image fusion framework provides great potential for lightening the complexity on the sensor side. Moreover, our presented algorithm achieves better results than compressive image fusion methods using only a single sparsifying transform in terms of both the subjective visual effect and objective evaluation metrics.

However, the compressive image fusion framework is just at its early stage. There are still many aspects to be further investigated. For example, we can see that the wavelet transform based compressive image fusion algorithm gives worse performance than the spatial finite-difference transform based algorithm. This observation may be because of the fact that weighted linear fusion rule based on the SD cannot provide an optimal composite measurements for the wavelet transform based compressive image fusion framework. So more advanced fusion rule for different sparsifying transform may be exploited by examining the underlying structure of the compressive measurements. Moreover, images contain many other features besides point-like and curve-like features. Thus we should find a dictionary that may sparsely represent all the features of images, using a dictionary training method such as K-SVD [24]. Finally, our algorithm may be accelerated by incorporating optimization techniques such as smoothing and more efficient line search.

TABLE 1 QUANTITATIVE ASSESSMENT OF FUSION RESULTS (M/N=30%)

Image	Method	MI	EP
Med	our presented	3.3018	0.4388
	TV	3.1035	0.4084
	wavelet	2.7769	0.3868
Clock	our presented	6.5759	0.5167
	TV	6.4920	0.4864
	wavelet	6.2392	0.4545

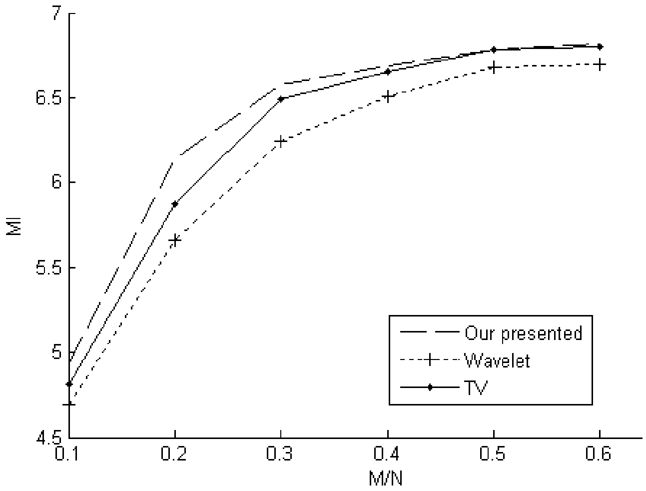

(a)

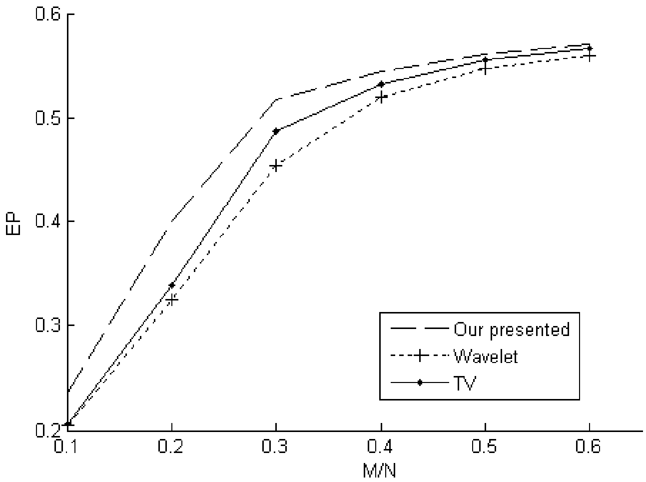

(b)

Figure 6. Objective metrics results using different methods for Clock: (a) mutual information (MI), (b) edge preservation (EP)

REFERENCES

[1] E. J. Candes, J. Romberg, and T. Tao, "Robust uncertainty principles: Exact signal reconstruction from highly incomplete frequency information," IEEE Transactions on Information Theory, vol. 52, no. 2, pp. 489-509, 2006. [Online]. Available: http://dx.doi.org/10.1109/TIT.2005.862083

[2] D. L. Donoho, "Compressed Sensing," IEEE Transactions on Information Theory, vol. 52, no. 4, pp. 1289-1306, 2006. [Online]. Available: http://dx.doi.org/10.1109/TIT.2006.871582

[3] M. B. Wakin, J. N. Laska, M. F. Duarte, et al. "An architecture for compressive imaging," IEEE International Conference on Image Processing, pp.1273-1276, 2006. [Online]. Available: http://dx.doi.org/10.1109/ICIP.2006.312577

[4] M. F. Duarte, M. A. Davenport, D. Takhar, et al. "Single-pixel imaging via compressive sampling," IEEE Signal Processing Magazine, vol. 25, no. 2, pp. 83-91, 2008. [Online]. Available: http://dx.doi.org/10.1109/MSP.2007.914730

[5] D. Giacobello, M. G. Christensen, M. N. Murthi, S. H. Jensen, and M. Moonen, "Retrieving Sparse Patterns Using a Compressed Sensing Framework: Applications to Speech Coding Based on Sparse Linear Prediction," IEEE Signal Processing Letters, vol. 17, no. 1, pp. 103-106, 2010. [Online]. Available: http://dx.doi.org/10.1109/LSP.2009.2034560

[6] D. Giacobello, M. G. Christensen, M. N. Murthi, S. H. Jensen, and M. Moonen, "Sparse linear prediction and its applications to speech processing," IEEE Transactions on Audio, Speech, and Language Processing, vol. 20, no. 5, pp. 1644-1657, 2012. [Online]. Available: http://dx.doi.org/10.1109/TASL.2012.2186807

[7] M., Fira, L., Goras, C., Barabasa, N., Cleju, "On ECG Compressed Sensing using Specific Overcomplete Dictionaries," Advances in Electrical and Computer Engineering, vol. 10, no. 4, pp. 23-28, 2010, doi:10.4316/AECE.2010.04004

[8] M., Fira, L., Goras, "A New Method for EEG Compressive Sensing," Advances in Electrical and Computer Engineering, vol. 12, no. 4, pp. 71-76, 2012, doi:10.4316/AECE.2012.04011

[9] J. Romberg, "Imaging via compressive sampling," IEEE Signal Processing Magazine, vol. 25, no. 2, pp. 14-20, 2008. [Online]. Available: http://dx.doi.org/10.1109/MSP.2007.914729

[10] T. Wan, N. Canagarajah, and A. Achim, "Compressive image fusion," IEEE International Conference on Image Processing, pp. 1308-1311, 2008. [Online]. Available: http://dx.doi.org/10.1109/ICIP.2008.4712003

[11] T. Wan, Z. C. Qin, "An application of compressive sensing for image fusion," International Journal of Computer Mathematics, vol. 88, no. 18, pp. 3915-3930, 2011. [Online]. Available: http://dx.doi.org/10.1080/00207160.2011.598229

[12] X. Li, S. Y. Qin, "Efficient fusion for infrared and visible images based on compressive sensing principle," IET Image Processing, vol. 5, no. 2, pp. 141-147, 2011. [Online]. Available: http://dx.doi.org/10.1049/iet-ipr.2010.0084

[13] X. Y. Luo, J. Zhang, J. Y. Yang, and Q. H. Dai, "Image fusion in compressed sensing," IEEE International Conference on Image Processing, pp. 2205-2208, 2009. [Online]. Available: http://dx.doi.org/10.1109/ICIP.2009.5413866

[14] X. Qu, X. Cao, D. Guo, C. Hu, and Z. Chen, "Combined sparsifying transforms for compressed sensing MRI," Electronics Letters, vol. 46, no. 2, pp. 121-123, 2010. [Online]. Available: http://dx.doi.org/10.1049/el.2010.1845

[15] M. A. T. Figueiredo, R. D. Nowak, and S. J. Wright, "Gradient projection for sparse reconstruction: application to compressed sensing and other inverse problems," IEEE Journal of Selected Topics in Signal Processing, vol. 1, no. 4, pp. 586-597, 2007. [Online]. Available: http://dx.doi.org/10.1109/JSTSP.2007.910281

[16] M. N. Do, M. Vetterli, "The contourlet transform: an efficient directional multiresolution image representation," IEEE Transactions on Image Processing, vol. 14, no. 12, pp. 1629-1632, 2005. [Online]. Available: http://dx.doi.org/10.1109/TIP.2005.859376

[17] Y. Lu, M. N. Do, "A new contourlet transform with sharp frequency localization," IEEE International Conference on Image Processing, pp. 1629-1632, 2006. [Online]. Available: http://dx.doi.org/10.1109/ICIP.2006.312657

[18] Q. Zhang, B. L. Guo, "Multifocus image fusion using the nonsubsampled contourlet transform," Signal Processing, vol. 89, no. 7, pp. 1334-1346, 2009. [Online]. Available: http://dx.doi.org/10.1016/j.sigpro.2009.01.012

[19] M. Lustig, D. Donoho, and J. M. Pauly, "Sparse MRI: the application of compressed sensing for rapid MR Imaging," Magnetic Resonance in Medicines, vol. 58, no. 10, pp. 1182-1195, 2007. [Online]. Available: http://dx.doi.org/10.1002/mrm.21391

[20] M. Lustig, D. L. Donoho, J. M. Santos, and J. M. Pauly, "Compressed sensing MRI," IEEE Signal Magazine, vol. 25, no. 2, pp. 72-82, 2008. [Online]. Available: http://dx.doi.org/10.1109/MSP.2007.914728

[21] W. W. Hager, H. Zhang. "A survey of nonlinear conjugate gradient methods," Pacific journal of Optimization, vol. 2, no. 1, pp. 35-58, 2006.

[22] G. H. Qu, D. L. Zhang, and P. F. Yan, "Information measure for performance of image fusion," Electronics Letters, vol. 38, no. 7, pp. 313-315, 2002. [Online]. Available: http://dx.doi.org/10.1049/el:20020212

[23] V. Petrovic, C. Xydeas, "On the effects of sensor noise in pixel-level image fusion performance," Proceedings of the Third International Conference on Information Fusion, vol. 2, pp. 14-19, 2010. [Online]. Available: http://dx.doi.org/10.1109/IFIC.2000.859842

[24] M. Aharon, M. Elad, and A. Bruckstein, "K-SVD: An algorithm for designing overcomplete dictionaries for sparse representation," IEEE Transactions on Signal Processing, vol. 54, no. 11, pp. 4311-4322, 2006. [Online]. Available: http://dx.doi.org/10.1109/TSP.2006.8811